Mutations in High-Voltage-Activated Calcium Channel Genes Stimulate Low-Voltage-Activated Currents in Mouse Thalamic Relay Neurons

Yi Zhang, Mayra Mori, Daniel L. Burgess, and Jeffrey L. Noebels

Developmental Neurogenetics Laboratory, Department of Neurology, Baylor College of Medicine, Houston, Texas 77030

Ca^{2+} currents, especially those activated at low voltages (LVA), influence burst generation in thalamocortical circuitry and enhance the abnormal rhythmicity associated with absence epilepsy. Mutations in several genes for high-voltage-activated (HVA) Ca^{2+} channel subunits are linked to spike-wave seizure phenotypes in mice; however, none of these mutations are predicted to increase intrinsic membrane excitability or directly enhance LVA currents. We examined biophysical properties of both LVA and HVA Ca^{2+} currents in thalamic cells of *tottering* (*tg*; Cav2.1/α1A subunit), *lethargic* (*lh*; β4 subunit), and *stargazer* (*stg*; γ2 subunit) brain slices. We observed 46, 51, and 45% increases in peak current densities of LVA Ca^{2+} currents evoked at -50 mV from -110 mV in *tg*, *lh*, and *stg* mice, respectively, compared with wild type. The half-maximal voltages for steady-state inactivation of LVA currents were shifted in a depolarized direction by 7.5–13.5 mV in all three mutants, although no alterations in the time-constant for recovery from inactivation of LVA currents were found. HVA peak current densities in *tg* and *stg* were increased by 22 and 45%, respectively, and a 5 mV depolarizing shift of the activation curve was observed in *lh*. Despite elevated LVA amplitudes, no alterations in mRNA expression of the genes mediating T-type subunits, Cav3.1/α1G, Cav3.2/α1H, or Cav3.3/α1I, were detected in the three mutants. Our data demonstrate that mutation of Cav2.1 or regulatory subunit genes increases intrinsic membrane excitability in thalamic neurons by potentiating LVA Ca^{2+} currents. These alterations increase the probability for abnormal thalamocortical synchronization and absence epilepsy in *tg*, *lh*, and *stg* mice.

Key words: Ca^{2+} currents; thalamocortical relay cells; absence seizures; stargazer; tottering; lethargic; calcium ion channel mutation

Rhythmic burst firing characterizes cellular signaling behavior in the thalamus and depends on intrinsic membrane properties of thalamocortical relay (TC) neurons, as well as the synaptically linked neurons in the adjacent thalamic reticular nucleus (nRT) (McCormick and Bal, 1997; Steriade, 2000). In both cell types, membrane hyperpolarization produces a Ca^{2+}-dependent low-threshold depolarization that serves as the generator potential for bursts of Na^{+} spikes (Llinás and Jahnsen, 1982). Voltage-clamp studies have identified the ion channel responsible for thalamic postinhibitory rebound burst firing as a T-type Ca^{2+} channel (Jahnsen and Llinás, 1984; Coulter et al., 1989a; Crunelli et al., 1989; Huguenard, 1996). Three genes, *Cacna1g*, *Cacna1h*, and *Cacna1i*, encoding T-type Cav3.1/α1G, Cav3.2/α1H, and Cav3.3/α1I α subunits have been localized in rat brain; Cav3.1 is predominantly expressed in thalamic relay nuclei and Cav3.3 in the nRT (Talley et al., 1999). The evidence directly linking this pathway to human absence epilepsy is based on thalamic involvement in spike-wave electrogenesis (Williams, 1953; Niedermeyer et al., 1969) and the ability of anti-absence drugs to reduce low-voltage-activated (LVA) currents (Coulter et al., 1989b; Gomora et al., 2001). Indirect evidence from experimental models provides additional support; LVA currents in nRT are increased in a rat model of absence epilepsy (Tsakiridou et al., 1995), and the threshold for spike-wave generation is significantly elevated in Cav3.1 $-/-$ mice (Kim et al., 2001).

The identification of mutations in Ca^{2+} channel subunit genes in *tottering* (*tg*; Cav2.1/α1A) (Fletcher et al., 1996), *lethargic* (*lh*; β_4) (Burgess et al., 1997), and *stargazer* (*stg*; γ_2) (Letts et al., 1998) mice and in humans (Escayg et al., 2000; Jouvenceau et al., 2001) that display an absence epilepsy phenotype provide an excellent opportunity to determine how defective Ca^{2+} signaling leads to thalamocortical epilepsy. In *tg* and its allele tg^{la}, dramatic reductions in single-channel open probability and peak current density of high-voltage-activated (HVA) P/Q-type (Cav2.1/2.2) Ca^{2+} currents in cerebellar Purkinje have been reported; however, it is difficult to explain how this defect could enhance intrinsic membrane excitability if present in the thalamocortical circuit (Dove et al., 1998; Lorenzon et al., 1998; Wakamori et al., 1998). In *lh* Purkinje cells, loss of functional β_4 subunits did not alter Cav2.1/2.2 Ca^{2+} currents, probably attributable to compensatory interactions with alternative β_{1-3} subunits (Burgess et al., 1999; McEnery et al., 1998). Similarly, loss of the γ_2 subunit in *stg*, shown recently to directly interact with HVA channels (Kang et al., 2001), had no significant effect on Ca^{2+} currents in cerebellar granule cells, presumably attributable to rearrangements with alternative members of the γ subunit family (Chen et al., 2000; Burgess et al., 2001).

Because the behavior of Ca^{2+} currents observed in cerebellar cells cannot be generalized to thalamic neurons, which express their own pattern of interacting subunits and modulatory signals, the cellular mechanisms of epileptogenesis in these three mutants remain unclear. We therefore evaluated the functional properties of both LVA and HVA Ca^{2+} currents in mutant thalamic neu-

Received Feb. 22, 2002; revised May 7, 2002; accepted May 10, 2002.

This work was supported by an American Epilepsy Society–Epilepsy Foundation Postdoctoral Fellowship (Y.Z.), National Institutes of Health Grant NS97209 (J.L.N.), and the Blue Bird Circle Foundation.

Correspondence should be addressed to Dr. Jeffrey L. Noebels, Department of Neurology, Baylor College of Medicine, One Baylor Plaza, Houston, TX 77030. E-mail: jnoebels@bcm.tmc.edu.

 0270-6474/02/226362-10$15.00/0

rons and examined *in vivo* gene expression patterns of the three LVA channel genes. Our results demonstrate that elevated thalamic LVA currents are a common feature shared by three distinct absence epilepsy gene mutations.

MATERIALS AND METHODS

Preparation of brain slices

Coronal brain slices (350-μm-thick) were prepared from 14- to 19-d-old homozygous wild-type (C57BL/6J), *tottering* (C57BL/6J-*Cacna1a*$^{tg/tg}$), *lethargic* (B6EiC3H-a/A-*Cacnβ4*$^{lh/lh}$), and *stargazer* (C57BL/6J-*Cacnγ2*$^{stg/stg}$) mice. Genotypes of the three mutants were confirmed by PCR of tail DNA (Burgess et al., 1997). Slices were obtained at the level of the lateral dorsal nucleus (LDN) of the thalamus, selected because of its projection to frontal cortical regions in which cortical spike-wave discharges in these mutants predominate (J. L. Noebels, unpublished observations). Each slice was perfused with a solution containing (in mM) (Kapur et al., 1998): 125 choline-Cl, 3.0 KCl, 1.25 NaH_2PO_4, 25 $NaHCO_3$, 1.0 $CaCl_2$, 7.0 $MgCl_2$, 10 dextrose, 1.3 ascorbate acid, and 3.0 pyruvate (bubbled with 95% O_2–5% CO_2). Slices were then incubated in an artificial CSF solution for 40 min at 37°C and then maintained at room temperature (22–25°C). The artificial CSF was gassed with 95% O_2–5% CO_2 and contained (in mM): 130 NaCl, 3.0 KCl, 2.0 $MgCl_2$, 2.0 $CaCl_2$, 1.25 NaH_2PO_4, 26 $NaHCO_3$, and 10 glucose.

Electrophysiological recording

Macroscopic Ca^{2+} currents from thalamocortical cells in the LDN were recorded using the whole-cell configuration of the patch-clamp technique. A Zeiss (Oberkochen, Germany) Axioskop fitted with a 40× water-immersion objective and differential interference contrast optics was used to view the slices and to identify neurons for analysis. Voltage command pulses were generated by a computer using pClamp 8.02 software. Currents were recorded with an Axopatch-1D amplifier, filtered at 10 kHz (−3 dB), and compensated for series resistance (~70%). Patch electrodes were drawn from borosilicate glass and coated with Sylgard. Ca^{2+} currents were corrected for leak and capacitive currents by subtracting a scaled current elicited by a 10 mV hyperpolarization from the standard holding potential of −70 mV. All recordings were performed at room temperature (22–25°C). The standard holding potential was −70 mV. To identify and stain the neurons in whole-cell recordings from the slice, 1% biocytin was included in the intracellular patch pipette solution. After recordings, the slices were cut into 50-μm-thick sections and then immediately fixed. A standard histochemical procedure was used to process the sections and stain the injected neurons (Huguenard and Prince, 1992).

Solutions. The recording bath solution consisted of (in mM): 115 NaCl, 3.0 KCl, 10 sucrose, 10 glucose, 26 $NaHCO_3$, 2 $MgCl_2$, 2.5 $CaCl_2$, 0.5 4-aminopyridine, 5 CsCl, 10 tetraethylammonium-Cl (TEA-Cl), and 0.001 TTX, pH 7.4 (gassed with 95% O_2–5% CO_2). The intracellular pipette solution contained (in mM): 78 Cs-gluconate, 20 HEPES, 10 BAPTA-Cs4 (cell-impermeant), 0.5 $CaCl_2$, 1.0 $MgCl_2$, 4 Mg-ATP, 0.3 GTP-Tris, 6 phosphocreatine (Di-Tris salt), 4.0 NaCl, and 20 TEA-Cl, pH 7.3 (titrated with CsOH).

Voltage protocols. To generate Ca^{2+} channel current–voltage (*I–V*) curves, currents were elicited by applying voltage step commands (200 msec) to varying potentials from a 3 sec prepulse potential at −60 or −110 mV. The *I–V* protocol for HVA Ca^{2+} currents consisted of voltage steps from −80 to +60 mV in 5 mV increments triggered from a 3 sec prepulse potential at −60 mV. To define LVA Ca^{2+} currents, difference currents obtained by digital subtraction of the currents elicited during depolarizing voltage steps from −60 and −110 mV were used. Standard voltage protocols for steady-state activation (SSA) of HVA Ca^{2+} currents, as well as the steady-state inactivation (SSI) and recovery from inactivation of LVA currents, respectively, were applied, and are explained in further detail below (see figure legends). In our study, we did not find any significant time-dependent ICa^{2+} run down within 30–40 min after membrane breaking. Statistical data analysis was tested by one-way ANOVA with the *post hoc* test. Differences with $p < 0.05$ were scored as statistically significant. The data shown represent means ± SE

In situ *hybridization*

In situ hybridization of mRNAs encoding α subunits for three calcium channel subtypes mediating LVA T-type Ca^{2+} currents, Cav3.1/α1G, Cav3.2/α1H, and Cav3.3/α1I, was performed in 2- to 3-week-old homozygous *tg*, *lh*, and *stg* mutants and C57BL/6 +/+ mice using standard techniques described previously in detail (Burgess et al., 1999). Briefly, horizontal brain sections (12-μm-thick) from 14- to 19-d-old mice were fixed in 4% paraformaldehyde in PBS and dehydrated through an ascending ethanol series. Antisense oligonucleotide probes were end labeled using terminal deoxynucleotidyl transferase (Promega, Madison, WI) and [α-^{35}S]dATP (1250 Ci/mmol; NEN, Boston, MA) to a specific activity of ~10^9 dpm/μg. The hybridization solution contained 50% (v/v) formamide, 4× SSC, 25 mM sodium phosphate, 1 mM sodium pyrophosphate, 10% dextran sulfate (w/v), 5× Denhardt's solution, 200 μg/ml sonicated herring sperm DNA (Promega), 100 μg/ml polyadenylic acid [5′] (Sigma-Aldrich, Milwaukee, WI), and 5 × 10^2 dpm of [α-^{35}S]dATP-labeled probe. Control sections were hybridized with an additional 100-fold excess of unlabeled oligonucleotide. The sequences of the 45-mer probes were as follows: *Cacna1g*, 5′-GATGCAGCTGGTGTCTGCTGGTTGGGAGTGAACAGACAAGATGG-3′; *Cacna1h*, 5′-CAAGAAGGTCAGGTTGTTGTTCCTGACGAAGGCGCTGTCCAGGAA-3′; and *Cacna1i*, 5′ GCGGATGGCTGACAGGTTGATGTTCTGTAGGTCCAGAGAGTACTC-3′. The probes were hybridized to the sections overnight at 42°C, washed in 1× SSC (22°C, 20 min), 0.3× SSC (55°C, 40 min), and 2× SSC (22°C, 5 min), and then dehydrated and exposed to Kodak BioMax MR film (Eastman Kodak, Rochester, NY) for 1 week. Developed autoradiographs were digitized (Sprintscan 35; Polaroid, Cambridge, MA) and arranged using Photoshop 5.0 (Adobe Systems, San Jose, CA), and all images were processed simultaneously. Optical density reflecting relative abundance of mRNA was determined by Scion (Frederick, MD) Image–NIH Image software. The *in situ* results were collected from wild-type and mutant mice (three animals per group). Eight brain sections were obtained from each group. Multiple small square areas within several anatomically distinct brain areas were selected, including the lateral dorsal nucleus and the adjacent white matter as an internal standard. These values were used to determine the lateral dorsal/white matter density ratio between affected mice and the respective homozygous wild-type mice. Differences in the optical densities were analyzed for statistical significance using Student's *t* test.

RESULTS

Increased peak current density of LVA calcium channels in TC neurons of *tottering*, *lethargic*, and *stargazer* mutants

We investigated the effects of mutation of Cav2.1/α1A (*tg*), β4 (*lh*), and γ2 (*stg*) Ca^{2+} channel subunits on Ca^{2+} currents in mouse LDN thalamic neurons defined by intracellular staining of biocytin. In mouse, these cells show a round-shaped cell body with multiple dendrites, similar in morphology to TC neurons from rat ventrobasal nucleus (Destexhe et al., 1998) (Fig. 1*A*). Figure 1*B* shows representative traces of LVA Ca^{2+} currents in response to a test pulse to −50 mV from a 3 sec prepulse to −110 mV in TC neurons from wild-type, *tg*, *lh*, and *stg* mice. At a membrane potential of −50 mV, all LVA Ca^{2+} currents have recovered from inactivation and are thus available for opening in both wild-type and mutant neurons (Figs. 2*B*, 3), whereas HVA Ca^{2+} currents in these cells have not yet started to activate (see Fig. 5*A*). The current traces of the LVA calcium channels show fast activation and inactivation, similar to those studied *in vitro* by expression of Cav3.1/α1G and Cav3.2/α1H T-type calcium channels (Lee et al., 1999; Delisle and Satin, 2000; Zhang et al., 2000), as well as native LVA currents from dissociated rat TC neurons (Destexhe et al., 1998). The peak current densities (i.e., normalized by cell capacitance) of LVA currents at a membrane potential of −50 mV increased by 46% in *tg*, 51% in *lh*, and 45% in *stg* mutants compared with control (Fig. 1*C*). The mean peak current amplitude and peak current density were −926.3 ± 182.2 pA and 9.5 ± 1.3 pA/pF in control, −1571.9 ± 106.8* pA and 17.63 ± 1.6** pA/pF in *tg*, −1852.1 ± 118.9** pA and 19.6 ± 1.0** pA/pF in *lh*, and 1514.9 ± 142* pA and 17.4 ± 1.2** pA/pF in *stg* mice (*$p < 0.05$; **$p < 0.01$ vs control).

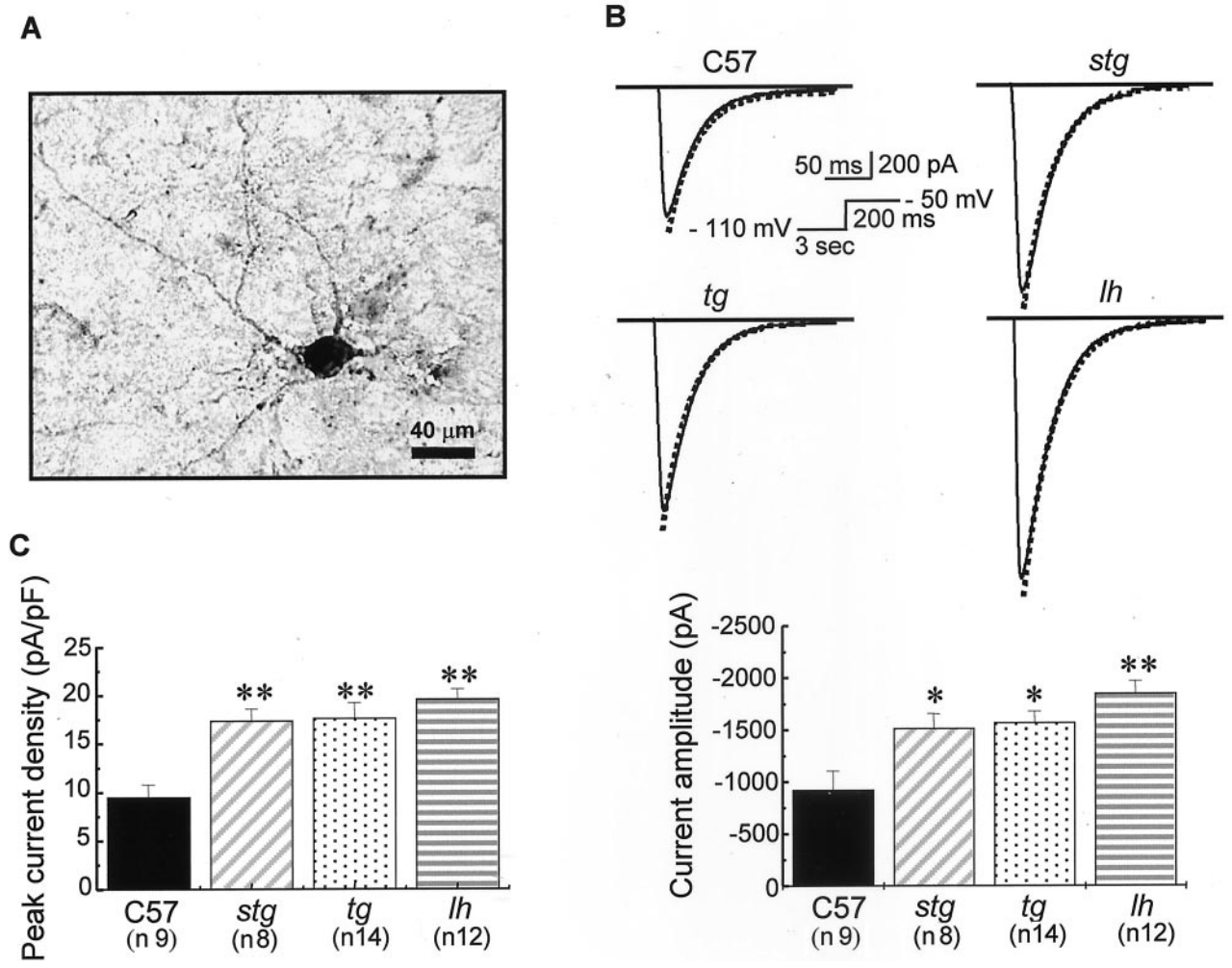

Figure 1. Increased LVA Ca^{2+} peak current in *tottering*, *lethargic*, and *stargazer*. *A*, Biocytin-filled thalamic neuron in the LDN of thalamus from wild-type mouse (C57BL/6J). *B*, Representative LVA current traces from TCs of the LDN in control, *tottering*, *lethargic*, and *stargazer* mice. The cell capacitance values of these four neurons were 101.25, 107.1, 95.5, and 95.34 pF, respectively. Holding potential, −70 mV. The membrane potential was prepulsed to −110 mV for 3 sec before stepping to −50 mV for 200 msec. Decay of the current was fitted by a single-exponential function (*dotted line*). No significant alterations in macroscopic current decay were found. The representative time constants τ for decay were 29.2, 29.7, 30.1, and 31.8 msec, respectively, in control, *tg*, *lh*, and *stg* mice. *C*, Elevated LVA Ca^{2+} current amplitude and peak current density from mutant TCs. LVA currents were evoked at the same membrane potential as described in *B*. The mean current amplitude and peak current densities were −926.3 ± 182.2 pA and 9.5 ± 1.3 pA/pF in control, 1514.9 ± 142 pA and 17.4 ± 1.2 pA/pF in *stg*, −1571.9 ± 106.8 pA and 17.63 ± 1.6 pA/pF in *tg*, and −1852.1 ± 118.9 pA and 19.6 ± 1.0 pA/pF in *lh* mice. $^{*}p < 0.05$; $^{**}p < 0.01$ versus control.

The duration of macroscopic inactivation for LVA Ca^{2+} currents in both control and mutant mice is closer to the time scale observed in Cav3.1 but not Cav3.2 T-type calcium channels expressed in mammalian cells (Lee et al., 1999; Zhang et al., 2000). The decay of macroscopic LVA currents evoked at −50 mV was fitted by a single-exponential function (Fig. 1*B*). No significant alterations in macroscopic LVA current decay were found in any of the three mutants compared with the wild type. The time constants for decay were 29.2, 29.7, 30.1, and 31.8, respectively, in control, *tg*, *lh*, and *stg* mice.

Depolarizing shifts in voltage dependence of steady-state inactivation and kinetics for recovery from inactivation of LVA currents

We next examined the kinetics of LVA Ca^{2+} currents in both wild-type and mutant neurons. The current traces of SSI of LVA are shown in Figure 2*A*. For the SSI protocol, we used a 4 sec prepulse to various membrane potentials before delivering a second test stimulus to −50 mV. The 4 sec prepulse was long enough to bring channels to a steady-state condition, because all LVA Ca^{2+} channels in TC neurons recover from inactivation within 3 sec (Fig. 3). As demonstrated in Figure 2*A*, LVA currents elicited at −50 mV from different premembrane potentials in both control and mutants show fast inactivation and decay completely within 150 msec. We did not observe any sustained component for current decay in *tg*, *lh*, or *stg* mice. Nevertheless, we found a significant depolarizing shift of the steady-state inactivation curves of LVA currents in the mutants in contrast to wild-type neurons (Fig. 2*B*). The mean half-maximal voltage ($V_{1/2}$) and slope (k) for SSI curves were −92.3 ± 0.16 and 6.8 ± 0.16 in control, −84.8 ± 0.17* and 6.51 ± 0.15 mV in *tg*, −78.72 ± 0.3** and 6.0 ± 0.27 mV in *lh*, and −78.6 ± 0.3** and 6.0 ± 0.27 mV in *stg*, respectively ($^{*}p < 0.05$; $^{**}p < 0.01$). The 7.5–13.5 mV depolarizing shifts of the voltage dependence for SSI of LVA currents in TC neurons of the mutants suggest that, at physiological membrane potentials varying from −70 to −75 mV, a higher

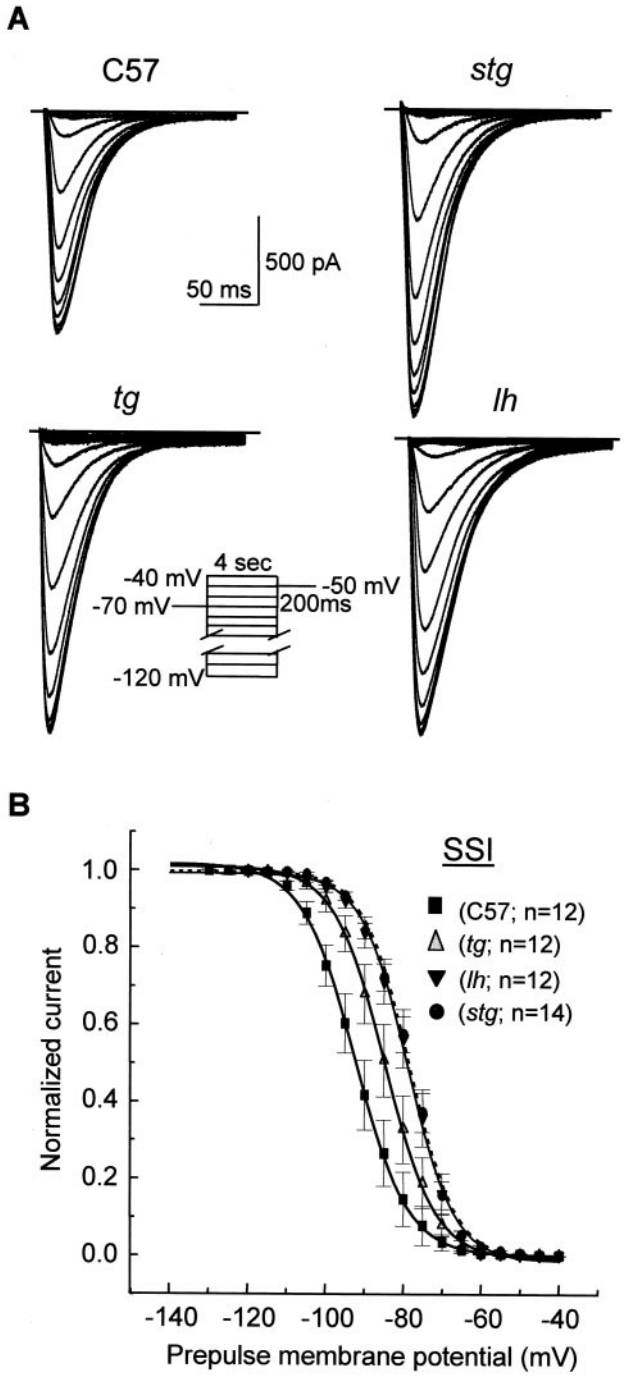

Figure 2. Depolarized shift of the voltage dependence of LVA calcium channel availability (steady-state inactivation) in *tottering*, *lethargic*, and *stargazer* mutants. *A*, Representative current traces for SSI of LVA Ca^{2+} currents. A standard double-pulse protocol for steady-state inactivation was given from the holding potential of −70 mV. A 4 sec prepulse at potentials ranging from −120 to −40 mV preceded each depolarization, followed by a subsequent voltage step to −50 mV for 200 msec. The interpulse interval was 10 sec. *B*, Normalized current–voltage curves for SSI of LVA Ca^{2+} currents. Current amplitude from the inactivation protocol, normalized to maximum, was plotted as a function of prepulse membrane potentials and best fitted with a Boltzmann function: $I/I_{max} = \{1 + \exp(V - V_{1/2})/k\} - 1$. The pooled half-maximal voltages ($V_{1/2}$) and slopes (k) were −92.3 ± 0.16 and 6.8 ± 0.16 mV in control, −84.8 ± 0.17* and 6.51 ± 0.15 mV in *tg*, −78.72 ± 0.3** and 6.0 ± 0.27 mV in *lh*, and −78.6 ± 0.3 ** and 6.0 ± 0.27 mV in *stg*, respectively. *$p < 0.05$; **$p < 0.01$.

fraction of all LVA calcium channels are available for opening in the mutant relative to control mice. Recovery from inactivation of the LVA Ca^{2+} currents in all mice was complete within 3 sec (Fig. 3). The recovery from inactivation curve was best fitted with a two-exponential function, and the fast and slow time constant derived from curve fitting did not significantly differ in any of the mutants compared with control mice. Thus, the depolarizing shift of SSI curves for LVA currents provides an additional biophysical mechanism that may contribute to increased neuronal burst synchronization observed in *tottering*, *lethargic*, and *stargazer* mice.

To determine whether the dramatic depolarizing shifts of SSI curves in all three mutants involves phosphorylation of thalamic T-type channels, we examined the effects of a specific protein kinase A inhibitor (PKA-I), as well as a protein kinase C inhibitor (PKC-I) on the voltage dependence of SSI for LVA currents. PKA-I at 50 μM (fragment 6–22, amide) or 100 μM PKC-I (fragment 19–36) was loaded into the pipette solution as described previously (Zhang et al., 2000), and the SSI protocol for LVA channels was then initiated 15–20 min after membrane rupture. We observed that neither PKA-I nor PKC-I antagonized the shift of $V_{1/2}$ for steady-state inactivation of the LVA currents found in untreated *tg*, *lh*, or *stg* mutants (data not shown). In addition, neither PKA-I nor PKC-I altered the baseline value of $V_{1/2}$ for SSI in untreated wild-type neurons, suggesting that the resting level of PKA or PKC could be low in both control and mutant mice. These observations suggest that neither PKA nor PKC significantly modulate the voltage dependence of SSI for LVA channels in these mutants, although consensus sites for both PKA and PKC exist on Cav3.1/α1G and Cav3.2/α1H channels (Cribbs et al., 1998; Perez-Reyes et al., 1998).

High-voltage-activated Ca^{2+} peak currents are increased in *tottering* and *stargazer* but not *lethargic* mice

We then determined whether mutation of Cav2.1/α1A (*tg*), β4 (*lh*), or γ2 (*stg*) Ca^{2+} channel subunits affect HVA Ca^{2+} currents in LDN cells. HVA Ca^{2+} currents are mediated by pore-forming α1 subunits, with current amplitude and gating regulated by cytoplasmic β subunits and transmembrane α2δ and γ subunits (Ahlijanian et al., 1990; Chien et al., 1995; Witcher et al., 1995; Gurnett et al., 1996; Walker and De Waard, 1998; Yamaguchi et al., 1998; Meir et al., 2000; Kang et al., 2001).

The *I–V* relationships of Ca^{2+} currents for control and three mutants are shown in Figure 5*A*. Figure 4 shows representative HVA Ca^{2+} current traces from wild-type, *tg*, *lh*, and *stg* mutant neurons. Both control and mutant HVA Ca^{2+} currents start to activate at approximately −45 mV. The currents reach a peak at −10 to −15 mV in control and mutant mice (Fig. 5*A*). Pooled peak currents and peak current densities are shown in Figure 5*B*. The mean peak current density was 10.12 ± 1.2, 13.03 ± 0.6**, 9.42 ± 0.4, and 17.99 ± 2.1** pA/pF in control, *tg*, *lh*, and *stg* (**$p < 0.01$ vs control). The mean peak amplitude was −885.51 ± 112.8, 1204.21 ± 86.4**, −901.3 ± 48.7, and −1567.6 ± 188** pA in control, *tg*, *lh*, and *stg* mutants, respectively (**$p < 0.01$ vs control).

Voltage dependence of steady-state activation for HVA currents

The steady-state activation curves of HVA Ca^{2+}currents in TC neurons are demonstrated in Fig 5*C*. The $V_{1/2}$ for steady-state

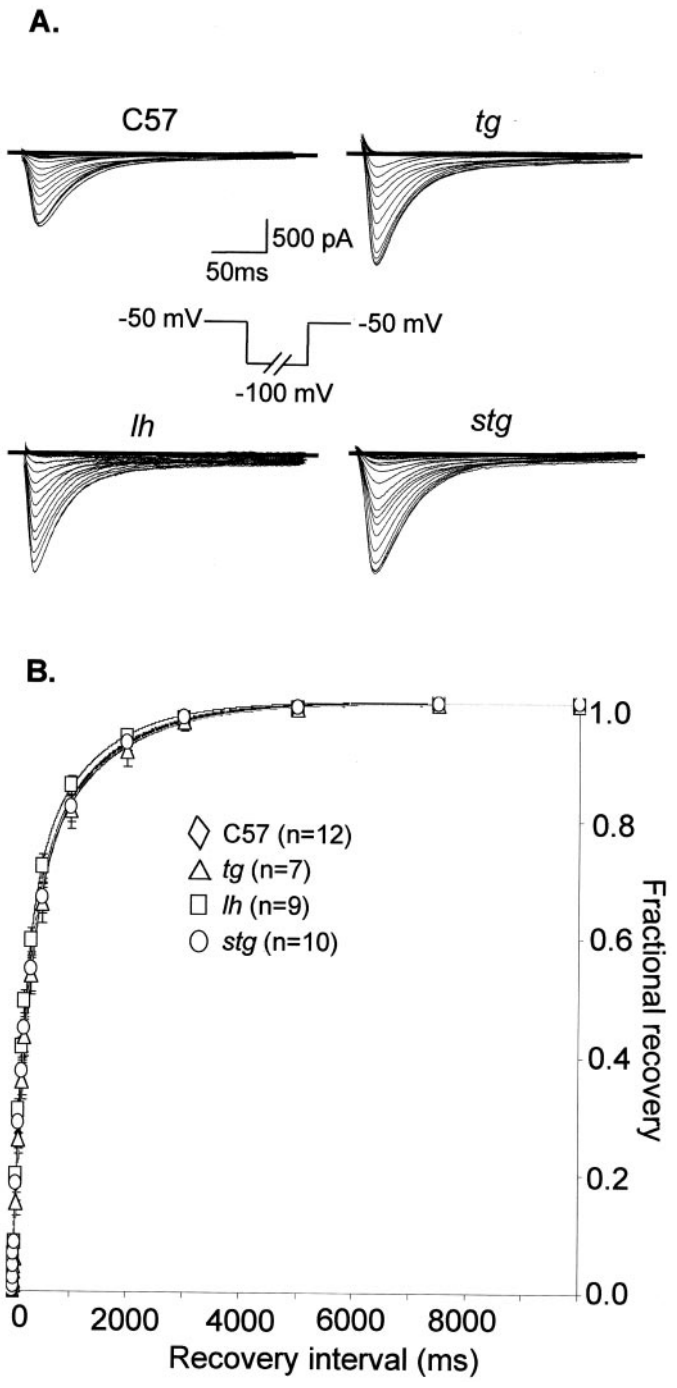

Figure 3. Recovery from inactivation of LVA Ca^{2+} currents. *A*, Representative current traces for recovery from inactivation of LVA currents in control, *tg*, *lh*, and *stg*. The holding potential was set to −50 mV, and 50 mV hyperpolarizations of incremental duration were applied. LVA peak amplitude was measured after returning to −50 mV. *B*, Recovery from inactivation curves. Recovery curves were established by plotting the normalized peak amplitude versus duration. The recovery curves followed a two-exponential time course, best fitted with fast time constant (τ_1) of 230, 240, 196, and 225 msec for control, *tg*, *lh*, and *stg*, and slow time constant (τ_2) of 1300, 1250, 1100, and 1270 msec for control, *tg*, *lh*, and *stg*, respectively.

activation of HVA currents in *tottering* and *stargazer* mutants did not change dramatically but shifted by 5 mV in a depolarized direction in *lethargic* mice relative to that in control. The mean values of $V_{1/2}$ and slope for SSA of HVA channels were −22.0 ± 0.17 and 5.5 ± 0.15 mV in control, −21.7 ± 0.16 and 4.5 ± 0.14 mV in *tg*, −17.0 ± 0.11* and 4.7 ± 0.1 mV in *lh*, and −23.9 ± 0.18 and 4.6 ± 0.16 mV in *stg*, respectively (*$p < 0.05$ vs control). The depolarized shift of the SSA curve in *lh* neurons is consistent with the *in vitro* finding that heterologous coexpression of β4 subunits elicited a hyperpolarizing shift for the SSA of Cav2.1 HVA calcium channels (De Waard and Campbell, 1995).

Expression of T-type Ca^{2+} channel Cav3.1/α1G mRNA in *tottering*, *lethargic*, and *stargazer* thalamus

To ascertain whether alterations in T-type calcium channel gene expression could underlie the increased LVA currents observed in mutant TC neurons, we compared regional mRNA expression levels of Cav3.1/α1G, Cav3.2/α1H, and Cav3.3/α1I. Figure 6 shows representative autoradiograms of coronal sections taken at the thalamic LDN level from mutant and wild-type brains. The three genes encoding neuronal T-type Ca^{2+} channels are expressed in distinct and primarily non-overlapping patterns that are consistent with localization patterns in adult rat brain (Talley et al., 1999). In wild-type mouse brain, Cav3.1 mRNA was expressed at high levels in thalamic relay nuclei, Cav3.3 mRNA was detected at high levels in nRT, and Cav3.2 mRNA was detected at only trace levels in either. No extrathalamic alterations were noted in any of the three mutants, and only the expression patterns of each gene in the thalamus are described.

Cav3.1/α1G mRNA

Transcripts of this gene were detected at highest levels in thalamic relay nuclei, with barely detectable levels present in nRT. This pattern was not appreciably altered in homozygous *tg*, *lh*, or *stg* mutant mice.

Cav3.2/α1H mRNA

Only barely detectable levels of Cav3.2 appeared in the wild-type thalamic relay nuclei, and trace levels were found in nRT. This pattern was not visibly altered in the *tg*, *lh*, or *stg* mutant mice.

Cav3.3/α1I mRNA

Cav3.3 was the most broadly distributed of the three T-type genes in the mouse thalamus, with high levels of mRNA observed in nRT. Low and barely detectable levels of Cav3.3 mRNA were detected in principle thalamic relay nuclei. The pattern of this gene was not appreciably altered in homozygous *tg*, *lh*, or *stg* mutant mice. Optical densitometry confirmed that there were no significant differences in optical densities of thalamic expression of Cav3.1–3 mRNA between the three mutants and the wild-type mice.

Although the correlation between mRNA intensity and LVA current density is unknown, the lack of appreciable differences in the *in situ* hybridization results between mutant and control provides no evidence to support the hypothesis that the Ca^{2+} channel subunit mutations in *tg*, *lh*, and *stg* mutants lead to functionally significant dysregulation of Cav3.1, Cav3.2, or Cav3.3 mRNA levels, and thus the ~50% increases in thalamic T-type Ca^{2+} currents cannot be simply accounted for by a proportional upregulation of channel gene expression.

DISCUSSION

Our results demonstrate increased peak current densities and a depolarizing shift of the steady-state inactivation curves of LVA currents, as well as subunit-specific HVA current modifications in *tottering*, *lethargic*, and *stargazer* thalamic neurons. The enhanced LVA currents could not be simply explained by major changes in

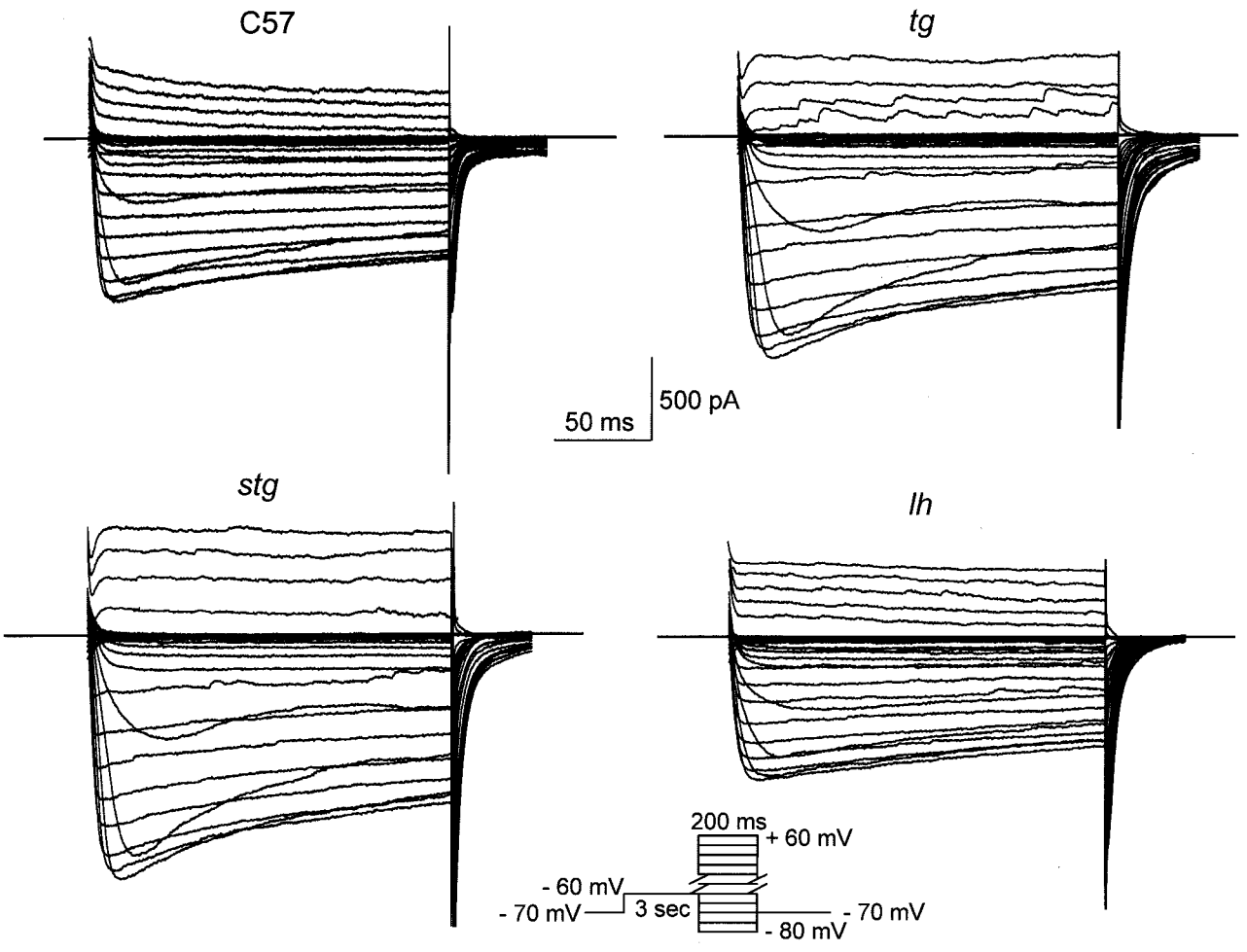

Figure 4. Representative superimposed HVA Ca^{2+} current traces from thalamocortical cells in control, *tg*, *lh*, and *stg* mice. The *I–V* protocol consisted of a 3 sec prepulse potential at −60 mV, followed by voltage steps (200 msec) ranging from −80 to +60 mV in 5 mV increments, with the holding potential maintained at −70 mV.

thalamic Cav3.1, Cav3.2, or Cav3.3 gene expression in any of the three mutants. Both the increased LVA current density and shifted voltage dependence of inactivation may favor spike-wave burst firing, the excitability phenotype shared by *tg*, *lh*, and *stg* mice. An additional finding was that HVA peak current densities, which may also facilitate network oscillations, are increased in *tg* and *stg* but not in *lh* thalamic neurons. This selectivity emphasizes the diversification of cellular compensatory mechanisms modulating Ca^{2+} currents after mutation of Cav2.1/α1A, β4, or γ2 Ca^{2+} channel subunits. Our study also provides a key mechanistic link between mutation of HVA subunits and the expression of thalamocortical hypersynchrony.

Functional properties of LVA Ca^{2+} channels in mutant thalamic neurons

The similarity of the spontaneous six to seven per sec spike-wave phenotype in *tg*, *lh*, and *stg* mice (Noebels and Sidman, 1979; Noebels et al., 1990; Hosford et al., 1992) suggests that a common cellular mechanism, potentiation of LVA currents, may be responsible for enhanced neuronal synchronization attributable to the distinct Ca^{2+} channel subunit mutations. LVA currents in thalamic neurons play a major and perhaps essential role in the genesis of synchronized oscillations in this system by amplifying postinhibitory high-frequency rebound bursting that enables rhythmic firing patterns. The HVA Ca^{2+} channel Cav2.1 and β4 subunits have not been shown to physically interact with T-type channel proteins or influence T-type channel biophysical properties in central neurons, although there is emerging evidence that γ2 may interact with both HVA and LVA channel types. Nonetheless, we found dramatic increases (45–51%) in peak current densities of thalamic LVA currents in all three mutants. The increases favor augmented burst firing and membrane hyperexcitability, because T-type channels start to activate at relatively hyperpolarized membrane potentials (Huguenard and Prince, 1992; Delisle and Satin, 2000; Zhang et al., 2000), and thalamic neurons have hyperpolarized resting membrane potentials attributable to the rhythmic inputs from GABAergic nRT neurons (Steriade and Llinás, 1988). In our study, LVA currents started to activate at approximately −65 to −70 mV (data not shown). Interestingly, we also observed a 7.5–13.5 mV depolarizing shift in SSI of LVA channels in all three mutants compared with the $V_{1/2}$ for SSI in wild-type mice. This very large depolarizing shift in SSI indicates a 7–30% elevation in LVA channel availability in the range of membrane potentials close to the resting membrane potential (−65 to −75 mV) (Fig. 2), and hence more channels will be open once the threshold for activation is reached.

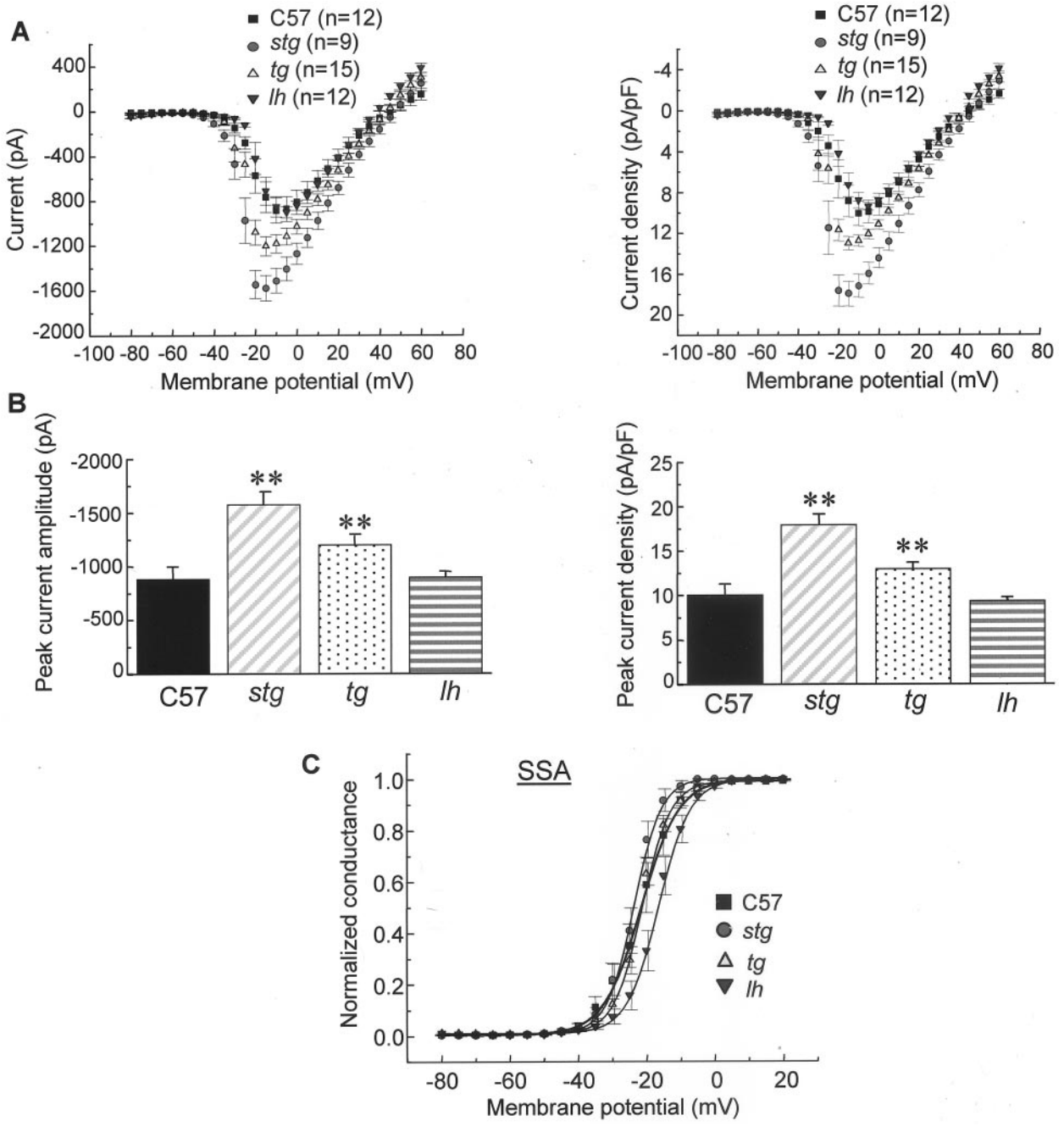

Figure 5. Peak HVA Ca^{2+} currents are increased in *tottering* and *stargazer* but not *lethargic* mice. *A*, Current density–voltage curves for HVA Ca^{2+} currents, constructed by plotting the normalized current amplitude at various membrane potentials. The voltage protocol used was identical to that described in Figure 4. *B*, Peak current density and current amplitude from *A*. The mean peak current density was 10.12 ± 1.2, 13.03 ± 0.6, 9.42 ± 0.4, and 17.99 ± 2.1 pA/pF in control, *tg*, *lh*, and *stg* (**$p < 0.01$ vs control). The mean current amplitude was −885.51 ± 112.8, 1204.21 ± 86.4, −901.3 ± 48.7, and −1567.6 ± 188 pA in control, *tg*, *lh*, and *stg* mutants (**$p < 0.01$ vs control). *C*, SSA of HVA Ca^{2+} currents in control, *tg*, *lh*, and *stg* mice. The steady-state conductance (G) and voltage (V) data were transformed from *I–V* data shown in *A*. The *solid* and *dotted curves* are fits of the data to the Boltzmann equation of the following form: $G/G_{max} = 1/(1 + \exp(V_{1/2} - V)/k)$, where G_{max} is maximum conductance, $V_{1/2}$ is half-maximal voltage, and k is the slope. The mean values of $V_{1/2}$ and slope for SSA of HVA currents are −22.0 ± 0.17 and 5.5 ± 0.15 mV in control, −21.7 ± 0.16 and 4.5 ± 0.14 mV in *tg*, −17.0 ± 0.11* and 4.7 ± 0.1 mV in *lh* mice, and −23.9 ± 0.18 and 4.6 ± 0.16 mV in *stg*, respectively (*$p < 0.05$ vs control).

Candidate mechanisms underlying LVA current alterations

We initially considered the possibility that peak LVA current increases might arise from additional *de novo* T-type channel synthesis, by either upregulation of native Cav3.1/α1G subunit expression or ectopic transcription of Cav3.2/α1H and Cav3.3/α1I subunits not normally expressed in these cells. Expression patterns of all three Ca_VT genes were unaltered, indicating that neither the mutant subunits nor the thalamocortical seizures they provoke are sufficient to induce Ca_VT gene transcription. The latter observation is consistent with the absence of c-Fos or c-Jun dysregulation in *stg* (Nahm and Noebels, 1998), confirming that the rhythmic oscillations during spike-wave synchronization are weak promoters of molecular plasticity compared with the pro-

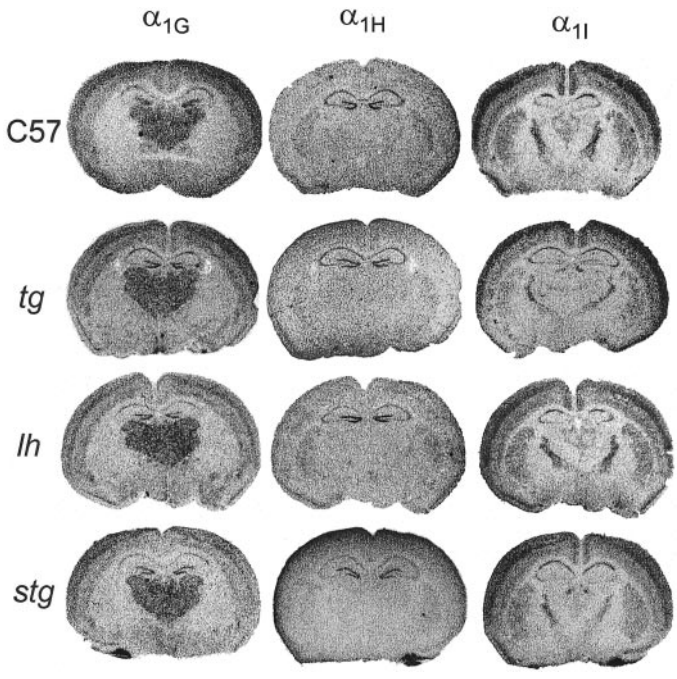

Figure 6. Expression of T-type calcium channel genes in *tg*, *lh*, and *stg* thalamus. The three genes, *Cacna1g* (Cav3.1/α1G), *Cacna1h* (Cav3.2/α1H), and *Cacna1i* (Cav3.3/α1I) were expressed in distinct and primarily non-overlapping patterns in coronal sections of mouse brain. Cav3.1 mRNA was detected at highest levels in neocortex and thalamus and in hippocampal dentate granule cells, with lower levels in hippocampal CA1–CA2 regions. Cav3.2 expression appeared to be restricted to hippocampal dentate gyrus and CA1–CA3 regions in the sections shown above. Cav3.3 expression was the most broadly distributed of the three T-type genes in mouse brain, with high levels of mRNA observed in nRT, habenula, hippocampal CA1 region, neocortex, and striatum. These patterns were not appreciably altered in homozygous *tg*, *lh*, or *stg* mutant mice.

longed, continuous depolarizations that stimulate expression of Ca^{2+} channels and other genes after convulsive seizures (Vigues et al., 1999). Although the increase in LVA peak current density detected in all three mutants is unlikely to result from altered Ca_VT gene expression, we cannot entirely exclude the possibility of persistent LVA channel elevation attributable to small increases of mRNA below the resolution of the method, increased mRNA translation efficiency, or decreased lability of the membrane protein. A mismatch between elevated LVA T-type Ca^{2+} currents and gene expression was observed previously in dissociated nRT neurons of the genetically undefined GAERS rat strain with absence epilepsy (Tsakiridou et al., 1995). In this model, one study detected no change in Cav3.1 expression (de Borman et al., 1999), whereas another reported small elevations of Cav3.1 mRNA in ventral posterior lateral thalamic relay nuclei and of Cav3.2 mRNA in nRT neurons (Talley et al., 2000).

Absence of thalamic Ca_VT gene upregulation suggests the existence of alternative nontranscriptional mechanisms for increased LVA current densities and shifted voltage dependence of SSI in *tg*, *lh*, and *stg* mutants. Because neither Cav2.1/α1A nor β4 proteins physically interact with Cav3.1/α1G subunits, the reduction of P/Q currents in *tg* and *lh* mutants must modify LVA current indirectly by altering a downstream Ca^{2+} signaling pathway. In the case of *stg* mice, direct interactions between γ2 and α1G may occur *in vivo*, and lack of regulatory γ2 subunits could directly alter current density and SSI by allowing novel γ3–8 subunit interactions with LVA channel complexes (Dolphin et al., 1999; Green et al., 2001; Rousset et al., 2001). Other potential mechanisms for elevated LVA current density include the contribution of depolarizing shifts of SSI, which increase channel availability, or increased membrane insertion of channels or spatial redistribution of channels from dendritic to somatic compartments in which they could affect the voltage dependence of inactivation and maximally influence firing properties (Karst et al., 1993). Finally, although we found little evidence for abnormal modulation of T-type channels in mutant neurons by PKA or PKC, modulation by PKG or through other pathways, including pH (Delisle and Satin, 2000; Shan et al., 2001), G-protein (Matsushima et al., 1993; Park and Dunlap, 1998), or molecules such as the endogenous cannabinoid anandamide (Chemin et al., 2001), remain possible candidate mechanisms.

Differential effects of Cav2.1/α1A, β4, and γ2 channel subunit mutations on HVA currents

We found that thalamic Ca^{2+} currents in *tg* brain slices showed a 22% increase in HVA peak current density, and a similar result was demonstrated recently in dissociated TCs of Cav2.1-deficient mutants (Song et al., 2001). Because point mutation or deletion of the Cav2.1 gene reduces or eliminates P-type currents (Dove et al., 1998; Wakamori et al., 1998; Jun et al., 1999), the small increase in whole-cell HVA peak current density observed in our experiment likely represents upregulation of other HVA currents, such as L-, N-, or R-type. Indeed, decreased Ca^{2+} currents through *tg* P/Q-type channels significantly increases mRNA levels for L-type Ca^{2+} channels in cerebellar Purkinje cells (Campbell and Hess, 1999). In TC neurons, we found that L-type currents account for 55–70% of whole-cell HVA currents in both control and the three mutants (data not shown). Additional pharmacological studies with selective Ca^{2+} channel blockers will define which specific HVA channels account for the increases in *tg* thalamic HVA currents.

The increased HVA Ca^{2+} peak current density in *stg* is consistent with recent functional analysis of γ2 subunit interactions with neuronal calcium channels, indicating that loss of the γ2 subunit may increase HVA currents (Letts et al., 1998; Klugbauer et al., 2000; Kang et al., 2001). These studies found that γ2/γ3 subunits cosedimented and coimmunoprecipitated with either Cav2.1/α1A or Cav2.2/α1B subunit from rabbit cerebellum and that γ2 coexpression in *Xenopus* oocytes significantly decreased the current amplitude of both Cav2.1 and Cav2.2 calcium channels. Of the neuronal Ca^{2+} channel γ subunits investigated so far, the γ2 and γ4 subunits shift the steady-state inactivation curve toward hyperpolarized potentials when coexpressed with Cav2.1 (Klugbauer et al., 2000). Thus, absence of γ2 in *stg* neurons should increase channel availability at membrane potentials (−40 to −30 mV) that start to activate HVA Ca^{2+} channels. Our data showed a 45% increase in HVA peak current density in TC neurons that is consistent with the non-neuronal expression studies.

In contrast to *tg* and *stg*, mutation of the β4 subunit did not significantly alter peak HVA current density in *lh* thalamic neurons. This result was unexpected, because β subunits regulate assembly and membrane incorporation of Cav2.1 subunits mediating HVA currents (Nishimura et al., 1993; Chien et al., 1995) and influence the amplitude of Ca^{2+} currents (De Waard and Campbell, 1995; Roche and Treistman, 1998) *in vitro*. β subunits have been also found to associate and functionally modify native P/Q-, L-, or N-type Ca^{2+} channels (Chien et al., 1995; Brice et

al., 1997; Meir et al., 2000). Interestingly, the lack of an effect on HVA peak current in TCs of *lh* mice is consistent with the same negative effect on P/Q-type Ca^{2+} currents in dissociated *lh* Purkinje cells (Burgess et al., 1999) and on P/Q channel function mediating transmitter release at *lh* hippocampal synapses (Qian and Noebels, 2000). Because alternative β subunits are widely localized in the brain, the negative impact of the $\beta 4$ mutation on thalamic HVA current in *lh* may be explained by β subunit reshuffling (Burgess et al., 1999). Finally, the 5 mV depolarizing shift of SSA found in *lethargic* mice is consistent with *in vitro* data that $\beta 4$ subunit interaction elicits a hyperpolarizing shift of inactivation curve for HVA currents (De Waard and Campbell, 1995). Because *lh* mice show both the LVA current increase and the spike-wave EEG phenotype, these findings suggest that the thalamic HVA alterations in *tg* and *stg* favor, but are not essential for, spike-wave generation.

In conclusion, our results are the first Ca^{2+} current defects to be described in *tg*, *lh*, and *stg* thalamic neurons and provide supportive physiological evidence for the functional interaction of β and γ regulatory subunits in modulating LVA currents.

REFERENCES

Ahlijanian MK, Westenbroek RE, Catterall WA (1990) Subunit structure and localization of dihydropyridine-sensitive calcium channels in mammalian brain, spinal cord, and retina. Neuron 6:819–832.

Brice NL, Berrow NS, Campbell V, Page KM, Brickley K, Tedder I, Dolphin AC (1997) Importance of the different beta subunits in the membrane expression of the alpha1A and alpha2 calcium channel subunits: studies using a depolarization-sensitive alpha1A antibody. Eur J Neurosci 9:749–759.

Burgess DL, Jones JM, Meisler MH, Noebels JL (1997) Mutation of the Ca^{2+}-channel β subunit gene *Cchb4* is associated with ataxia and seizures in the lethargic (*lh*) mouse. Cell 88:385–392.

Burgess DL, Biddlecome GH, McDonough SI, Diaz ME, Zilinski CA, Bean BP, Campbell KP, Noebels JL (1999) β subunit reshuffling modifies N- and P/Q type Ca^{2+} channel subunit compositions in lethargic mouse brain. Mol Cell Neurosci 13:293–311.

Burgess DL, Gefrides LA, Foreman PJ, Noebels JL (2001) A cluster of three novel Ca^{2+} channel gamma subunit genes on chromosome 19q13.4: evolution and expression profile of the gamma subunit gene family. Genomics 71:339–350.

Campbell DB, Hess EJ (1999) L-type calcium channels contribute to the tottering mouse dystonic episodes. Mol Pharmacol 55:23–31.

Chemin J, Monteil A, Perez-Reyes E, Nargeot J, Lory P (2001) Direct inhibition of T-type calcium channels by the endogenous cannabinoid anadamide. EMBO J 20:7033–7040.

Chen L, Chetkovich DM, Petralia RS, Sweeney NT, Kawasaki Y, Wenthold RJ, Bredt DS, Nicoll RA (2000) Stargazin regulates synaptic targeting of AMPA receptors by two distinct mechanisms. Nature 408:936–943.

Chien AL, Zhao X, Shirokov RE, Puri TS, Chang CF, Sun D, Rios E, Hosey MM (1995) Role of a membrane-localized β subunit in the formation and targeting of functional L-type Ca^{2+} channels. J Biol Chem 270:30036–30044.

Coulter DA, Huguenard JR, Prince DA (1989a) Calcium currents in rat thalamocortical relay neurons: kinetic properties of the transient, low-threshold current. J Physiol (Lond) 414:587–604.

Coulter DA, Huguenard JR, Prince DA (1989b) Characterization of ethosuximide reduction of low-threshold calcium current in thalamic neurons. Ann Neurol 25:582–593.

Cribbs LL, Lee J-H, Yang J, Satin J, Zhang Y, Daud A, Barclay J, Williamson MP, Fox M, Rees M, Perez-Reyes E (1998) Cloning and characterization of α_{1H} from human heart, a member of the T-type calcium channel gene family. Circ Res 83:103–109.

Crunelli V, Lightowler S, Pollard CE (1989) A T-type Ca^{2+} current underlies low-threshold Ca^{2+} potentials in cells of the cat and rat lateral geniculate nucleus. J Physiol (Lond) 413:543–561.

de Borman B, Lakaye B, Minet A, Zorzi W, Vergnes M, Marescaux C, Grisar T (1999) Expression of mRNA encoding alpha1E and alpha1G subunit in the brain of a rat model of absence epilepsy. NeuroReport 10:569–574.

Delisle BP, Satin J (2000) pH Modulation of human T-type calcium channel gating. Biophys J 78:1895–1905.

Destexhe A, Neubig M, Ulrich D, Huguenard J (1998) Dendritic low-threshold currents in thalamic relay cells. J Neurosci 18:3574–3588.

De Waard M, Campbell KP (1995) Subunit regulation of the neuronal α_{1A} Ca^{2+} channel expressed in *Xenopus* oocytes. J Physiol (Lond) 485:619–634.

Dolphin AC, Wyatt CN, Richards J, Beattie RE, Craig P, Lee J-H, Cribbs LL, Volsen SG, Perez-Reyes E (1999) The effect of $\alpha 2$-δ and other accessory subunits on expression and properties of the calcium channel $\alpha 1G$. J Physiol (Lond) 519:35–45.

Dove LS, Abbott LC, Griffith WH (1998) Whole-cell and single channel analysis of P-type calcium currents in cerebellar Purkinje cells of leaner mutant mice. J Neurosci 18:7687–7699.

Escayg A, De Waard M, Lee DD, Bichet D, Wolf P, Mayer T, Johnston J, Baloh R, Sander T, Meisler MH (2000) Coding and noncoding variation of the human calcium channel beta4-subunit gene CACANB4 in patients with idiopathic generalized epilepsy and episodic ataxia. Am J Hum Genet 66:1531–1539.

Fletcher CF, Lutz CM, O'Sullivan TN, Shaughnessy JDJ, Hawkes R, Frankel WN, Copeland NG, Jenkins NA (1996) Absence epilepsy in tottering mutant mice is associated with calcium channel defects. Cell 87:607–617.

Gomora JC, Daud AN, Weiergraber M, Perez-Reyes E (2001) Block of cloned human T-type calcium channels by succinimide antiepileptic drugs. Mol Pharmacol 60:1121–1132.

Green PJ, Warre R, Hayes PD, McNaughton NC, Medhurst AD, Pangalos M, Duckworth DM, Randall AD (2001) Kinetic modification of the alpha(1I) subunit-mediated T-type Ca^{2+} channel by a human neuronal Ca^{2+} channel gamma subunit. J Physiol (Lond) 533:467–478.

Gurnett CA, De Waard M, Campbell KP (1996) Dual function of the voltage-dependent Ca^{2+} channel alpha 2 delta subunit in current stimulation and subunit interaction. Neuron 16:431–440.

Hosford DA, Clark S, Cao Z, Wilson Jr WA, Lin FH, Morrisett RA, Huin A (1992) The role of $GABA_B$ receptor activation in absence seizures of lethargic (*lh*/*lh*) mice. Science 257:398–401.

Huguenard JR (1996) Low-threshold calcium currents in central nervous system neurons. Annu Rev Physiol 58:329–348.

Huguenard JR, Prince DA (1992) A novel T-type current underlies prolonged Ca^{2+}-dependent bursts in GABAergic firing neurons of rat thalamic reticular nucleus. J Neurosci 12:3804–3817.

Jahnsen H, Llinás RR (1984) Ionic basis for the electroresponsiveness and oscillatory properties of guinea-pig thalamic neurons in vitro. J Physiol (Lond) 349:227–247.

Jouvenceau A, Eunson LH, Spauschus A, Ramesh V, Zuberi SM, Kullmann DM, Hanna MG (2001) Human epilepsy associated with dysfunction of the brain P/Q-type calcium channel. Lancet 358:801–807.

Jun K, Piedras-Renteria ES, Smith SM, Wheeler DB, Lee SB, Lee TG, Chin H, Adams ME, Scheller RH, Tsien RW, Shin HS (1999) Ablation of P/Q-type Ca channel currents, altered synaptic transmission, and progressive ataxia in mice lacking the a1A-subunit. Proc Natl Acad Sci USA 96:15245–15250.

Kang MG, Chen CC, Felix R, Letts VA, Frankel WN, Mori Y, Campbell KP (2001) Biochemical and biophysical evidence for gamma 2 subunit association with neuronal voltage-activated Ca^{2+} channels. J Biol Chem 276:32917–32924.

Kapur A, Yeckel MF, Gray R, Johnston D (1998) L-type calcium channels are required for one form of hippocampal mossy fiber LTP. J Neurophysiol 79:2181–2190.

Karst H, Joels M, Wadman WJ (1993) Low-threshold calcium current in dendrites of the adult rat hippocampus. Neurosci Lett 164:154–158.

Kim D, Song I, Keum S, Lee T, Jeong MJ, Kim SS, McEnery MW, Shin HS (2001) Lack of the burst firing of thalamocortical relay neurons and resistance to absence seizures in mice lacking alpha(1G) T-type Ca^{2+} channels. Neuron 31:35–45.

Klugbauer N, Dai S, Specht V, Lacinova L, Marais E, Bohn G, Hofmann FJ (2000) A family of gamma-like calcium channel subunits. FEBS Lett 470:189–197.

Lee J-H, Daud AN, Cribbs LL, Lacerda AE, Pereverzev A, Klockner U, Schneider T, Perez-Reyes E (1999) Cloning and expression of a novel member of the low voltage-activated T-type calcium channel family. J Neurosci 19:1912–1921.

Letts VA, Felix R, Biddlecome GH, Arikkath J, Mahaffey CL, Valenzuela A, Bartlett FS, Mori Y, Campbell KP, Frankel WN (1998) The mouse stargazer gene encodes a neuronal Ca^{2+} channel gamma subunit. Nat Genet 19:340–347.

Llinás R, Jahnsen H (1982) Electrophysiology of mammalian thalamic neurons in vitro. Nature 297:406–408.

Lorenzon NM, Lutz CM, Frankel WN, Beam KG (1998) Altered calcium channel currents in Purkinje cells of the neurological mutant mouse leaner. J Neurosci 18:4482–4489.

Matsushima T, Tegner J, Hill RH, Grillner S (1993) GABAB receptor activation causes a depression of low- and high-voltage-activated Ca^{2+} currents, postinhibitory rebound, and postspike afterhyperpolarization in lamprey neurons. J Neurophysiol 70:2606–2619.

McCormick DA, Bal T (1997) Sleep and arousal: thalamocortical mechanisms. Annu Rev Neurosci 20:185–215.

McEnery MW, Copeland TD, Courtney LV (1998) Altered expression and assembly of N-type calcium channel $\alpha 1_\beta$ and β subunits in epileptic lethargic (lh/lh) mouse. J Biol Chem 273:21435–21438.

Meir A, Dell DC, Stephens GL, Page KM, Dolphin AC (2000) Calcium channel beta subunit promotes voltage-dependent modulation of alpha1B by G beta gamma. Biophys J 79:731–746.
Nahm WK, Noebels JL (1998) Nonobligate role of early or sustained expression of immediate-early gene proteins c-Fos, c-Jun, and Zif/268 in hippocampal mossy fiber sprouting. J Neurosci 18:9245–9255.
Niedermeyer E, Laws Jr ER, Walker EA (1969) Depth EEG findings in epileptics with generalized spike-wave complexes. Arch Neurol 21:51–58.
Nishimura S, Takeshima H, Hofmann F, Flockerzi V, Imoto K (1993) Requirement of the calcium channel β subunit for functional conformation. FEBS Lett 324:283–286.
Noebels JL, Sidman RL (1979) Inherited epilepsy: spike-wave and focal motor seizures in the mutant mouse yottering. Science 204:1334–1336.
Noebels JL, Qiao X, Bronson RT, Spencer C, Davisson MT (1990) Stargazer: a new neurological mutant on chromosome 15 in the mouse with prolonged cortical seizures. Epilepsy Res 7:129–135.
Park D, Dunlap K (1998) Dynamic regulation of calcium influx by G-proteins, action potential waveform, and neuronal firing frequency. J Neurosci 18:6757–6766.
Perez-Reyes E, Cribbs LL, Daud A, Lacerda AE, Barclay J, Williamson MP, Fox M, Rees M, Lee J-H (1998) Molecular characterization of a neuronal low-voltage-activated T type calcium channel. Nature 391:896–900.
Qian J, Noebels JL (2000) Presynaptic Ca^{2+} influx at a mouse central synapse with Ca^{2+} channel subunit mutations. J Neurosci 20:163–170.
Roche JP, Treistman SN (1998) The Ca^{2+} channel beta3 subunit differentially modulate G-protein sensitivity of alpha1A and alpha1B. J Neurosci 18:878–886.
Rousset M, Cens T, Restituito S, Barrere C, Black III JL, McEnery MW, Charnet P (2001) Functional roles of gamma2, gamma3 and gamma4, three new Ca^{2+} channel subunits, in P/Q-type Ca^{2+} channel expressed in *Xenopus* oocytes. J Physiol (Lond) 532:583–593.
Shan MJ, Meis S, Munsch T, Pape HC (2001) Modulation by extracellular pH of low- and high-voltage-activated calcium currents of rat thalamic relay neurons. J Neurophysiol 85:1051–1058.
Song I, Kim D, Jun K, Shin HS (2001) Role of T-type calcium channels in the genesis of absence seizure in the mutant mice for α_{1A}, the pore-forming subunit of the P/Q-type calcium channel. Soc Neurosci Abstr 27:151.21.
Steriade M (2000) Corticothalamic resonance, states of vigilance and mentation. Neuroscience 101:243–276.
Steriade M, Llinás RR (1988) The functional states of the thalamus and the associated neuronal interplay. Physiol Rev 68:649–742.
Talley EM, Cribbs LL, Lee JH, Daud A, Perez-Reyes E, Bayliss DA (1999) Differential distribution of three members of a gene family encoding low voltage-activated (T-type) calcium channels. J Neurosci 19:1895–1911.
Talley EM, Solorzano G, Depaulis A, Perez-Reyes E, Bayliss DA (2000) Low-voltage-activated calcium channel subunit expression in a genetic model of absence epilepsy in the rat. Mol Brain Res 75:159–165.
Tsakiridou E, Bertollini L, de Curtis M, Avanzini G, Page HC (1995) Selective increase in T-type calcium conductance of reticular thalamic neurons in a rat model of absence epilepsy. J Neurosci 15:3110–3117.
Vigues S, Gastaldi M, Chabret C, Massacrier A, Cau P, Valmier J (1999) Regulation of calcium channel alpha(1A) subunit splice variant mRNAs in kainate-induced temporal lobe epilepsy. Neurobiol Dis 6:288–301.
Wakamori M, Yamazaki K, Matsunodaira H, Teramoto T, Tanaka I, Niidome T, Sawada K, Nishizawa Y, Sekiguchi N, Mori E, Mori Y, Imoto K (1998) Single tottering mutations responsible for the neuropathic phenotype of the P-type calcium channel. J Biol Chem 273:34857–34867.
Walker D, De Waard M (1998) Subunit interaction sites in voltage-dependent Ca^{2+} channels: role in channel function. Trends Neurosci 21:148–154.
Williams DA (1953) A study of thalamic and cortical rhythms in petit mal. Brain 76:50–69.
Witcher DR, De Waard M, Liu H, Pragnell M, Campbell KP (1995) Association of native β Ca^{2+} channel subunits with the α subunit interaction domain. J Biol Chem 270:18088–18093.
Yamaguchi H, Hara M, Strobeck M, Fukasawa K, Schwartz A, Varadi G (1998) Multiple modulation pathways of calcium channel activity by a β subunit participaiton in membrane trafficking of the subunit. J Biol Chem 273:19348–19356.
Zhang Y, Cribbs LL, Satin J (2000) Arachidonic acid modulation of α1H, a cloned human T-type calcium channel. Am J Physiol Heart Circ Physiol 278:H184–H193.